Tackling proteome changes in the *longissimus thoracis* bovine muscle in response to pre-slaughter stress

Daniel Franco[a], *Ariadna Mato*[b], *Francisco J. Salgado*[c], *María López-Pedrouso*[b],

Mónica Carrera[d], *Susana Bravo*[e], *María Parrado*[b], *José M. Gallardo*[d], *Carlos Zapata*[b,*]

[a]*Meat Technology Center of Galicia, r/ Galicia 4, Parque Tecnolóxico de Galicia, San Cibrao das Viñas, Ourense-32900, Galicia-Spain*

[b]*Department of Genetics, University of Santiago de Compostela, Santiago de Compostela-15782, Spain*

[c]*Department of Biochemistry and Molecular Biology, University of Santiago de Compostela, Santiago de Compostela-15782, Spain* [d]*Spanish National Research Council (CSIC), Marine Research Institute (IIM), Eduardo Cabello 6, Vigo-36208, Pontevedra, Spain* [e]*Proteomics Laboratory, CHUS, Santiago de Compostela-15782, Spain*

Corresponding author. Fax: + 34 981528006.

E-mail address: c.zapata@usc.es (C. Zapata).

ABSTRACT:

Pre-slaughter stress has adverse effects on meat quality that can lead to the occurrence of Dark Firm Dry (DFD) meat in cattle. This study explores the previously uncharacterized proteome changes linked to pre-slaughter stress in the *longissimus thoracis* (LT) bovine muscle. Differential proteome profiles of DFD and normal (non-DFD) LT meat samples from male calves of the Rubia Gallega breed were assessed by 2-DE coupled to MS analysis (LC-MS/MS and MALDI TOF/TOF MS). A total of seven structural-contractile proteins (three different myosin light chain isoforms, two fast skeletal myosin light chain 2 isoforms, troponin C type 2 and cofilin-2) and three metabolism enzymes (triosephosphate isomerase, ATP synthase and beta-galactoside alpha-2,6-sialyltransferase) were found to have statistically significant differential abundance in sample groups. In addition, 2-DE in combination with the phosphoprotein-specific fluorescent dye Pro-Q DPS revealed that highly phosphorylated fast skeletal myosin regulatory light chain 2 isoforms underwent the most intense relative change in muscle conversion to DFD meat. Therefore, they appear to be the most sensitive biomarkers of stress just prior to slaughter in Rubia Gallega. Overall, these findings will facilitate a more integrative understanding of the biochemical processes associated with stress in cattle muscle and their effects in meat quality.

Biological significance: Pre-slaughter stress is a crucial factor in meat production. Animals destined for slaughter are stressed by a variety of endogenous and exogenous factors that negatively affect the complex post-mortem biochemical events underlying the conversion of muscle into

meat. The study of the muscle proteome has a great relevance for understanding the molecular mechanisms associated with stress. However, there is no information available on the molecular changes linked to pre-slaughter stress in cattle on the proteome scale. Our study led to the identification of a number of candidate proteins associated with the response to pre-slaughter stress in the LT bovine muscle of the Rubia Gallega breed. The functions of those significantly changed proteins have a clear biological relationship with stress response. These findings contribute to a deeper insight into the molecular pathways that respond to stress in cattle.

Keywords: Pre-slaughter stress, biomarkers, *Bos taurus,* DFD meat, *Longissimus thoracis,* Proteome, Relative change measure

1. Introduction

Pre-slaughter stress (PSS) is a very complex trait conditioned by a variety of endogenous (e.g. sex, genetics and age) and exogenous animal factors linked to pre-slaughter transport and handling activities [1,2]. Exogenous animal stressors include practices of loading and unloading, human presence, changes in social structure through separation and mixing with strange animals, feed and water deprivation during transportation, lairage in slaughter house and exposure to new and unfamiliar environment. PSS has serious adverse effects on animal welfare [3,4] and causes detrimental effects to the biochemical processes that occur during the transformation of muscle into meat [5,6]. Thus, exposing cattle to PSS can lead to the formation of Dark Firm Dry (DFD) meat due to depletion of muscle glycogen reserves and the accumulation of lactic acid that alters the normal process of post-mortem acidification of meat, affecting decisive factors of final meat quality such as tenderness, juiciness, color and flavor [5–7].

DFD meat occurs when the ultimate pH post-mortem measured after 12-48 hours is higher than 6.0 [8]. The elevated pH is associated with relatively little denaturation of proteins, water is tightly bound and little or no exudates are expelled [6]. Consequently, this type of meat has poor processing characteristics, darker color [9], great variations in tenderness and high water-holding capacity [10] and high potential of spoilage at an early age [11] compared to normal meat. It can also be inferior in flavor and consumer acceptability [12]. The incidence of DFD in meat varies markedly over different countries, often with rates of about 10%, and is the cause of large economic losses [5,8,13,14].

A number of biochemical parameters, indicators of perimortem (plasma and/or urinary levels of cortisol, adrenaline, noradrenaline, catecholamines,

etc.) and post-mortem muscle metabolism (pH, lactate, glycogen, etc.), are tradition- ally used to evaluate the stress status of animals at slaughter [15–17]. However, the occurrence of DFD meat provides an excellent opportunity to obtain insight into the structural and regulatory proteins that directly affect muscle in response to PSS and their influence on meat quality. The use of proteo- mics has opened new and promising avenues for tackling control quality and product safety in the meat industry [18–20]. Reference map of beef muscle proteome and its differentiation over different scenarios have already been established on the basis of 2-DE coupled with MS analyses [21–27]. Intensive proteomic and functional analyses have been particularly addressed to assess the biochemical mechanisms underlying tenderization processes of meat, one of the most important factors contributing to meat quality [19,22,25,26,28–31]. To our knowledge, no previous systematic research has been addressed to evaluate proteome changes due to stress with adverse effects on meat quality in cattle.

This study is a first attempt to unravel stress-dependent proteome changes in beef muscle. Specifically, we have studied proteome changes in the *longissimus thoracis* muscle in response to PSS from male calves of the Rubia Gallega breed. This study opens the way towards a better understanding of the molecular mechanisms linked to stress in cattle and their accompanying effects on meat quality.

2. Materials and methods

2.1. Animals, sample preparation and experimental design

Proteome changes linked to PSS in cattle were studied in animals that experienced the usual practices in the Spanish beef industry. The occurrence of DFD meat was used as indicator of animals affected by PSS.

A total of four biological replicates of DFD and control (normal or non-DFD) meats from male calves of the Rubia Gallega breed (Spain) were used in this study. Meat samples were selected according to discriminatory meat quality parameters between DFD and normal meat, in a total of 76 male calves. Therefore, the incidence of DFD meat in our study was 5.3%. Animals with a mean age of 10 months were transported from family farms to the abattoir the day before slaughter, stunned with a captive bolt, slaughtered and dressed according to European Union regulations (Council Directive 93/119/EEC), in an accredited abattoir (Lugo, Spain). Control samples were obtained from the same farm and slaughtered the same day as DFD samples in order to homogenize the experimental conditions over sample groups. Carcasses were chilled for 24 h in a refrigerated chamber at 2 °C and relative humidity of 98%. At this point, the *longissimus thoracis* (LT) muscle was excised from the left half of each carcass. Two 2.5 cm thick steak taken at the fifth rib were packed under vacuum conditions and transported under refrigerated conditions. The first steak was used for pH and color determination and proteome analysis; the second one to assess water holding capacity and textural tests. Samples for proteome analysis were lyophilized under optimal conditions as previously described [32] and subsequently frozen at -80 °C until required, whereas samples for water holding capacity and texture determinations were analyzed immediately.

2.2. Determination of meat quality parameters

The pH of the samples was measured using a digital portable pH-meter (Hanna Instruments, Eibar) equipped with a penetration probe. A portable colorimeter (Konica Minolta CM-600d, Osaka) with the following machine settings (pulsed xenon arc lamp, angle of 0° viewing angle geometry,

standard illuminant D65 and aperture size of 8 mm) was used to measure the meat color in the CIELAB space [lightness (L*), redness (a*) and yellowness (b*)]. Three measurements were performed for each sample in homogeneous and representative areas, free of intramuscular fat. The water holding capacity (WHC) was measured as cooking loss. Steaks were cooked placing vacuum package bags in a water bath with automatic temperature control (JP Selecta, Precisdg, Barcelona) until they reached an internal temperature of 70 °C, controlled by thermocouples type K (Comark, PK23M, Norwich), and connected to a data logger (Comark Dilligence EVG, N3014, Norwich). After cooking, samples were cooled in a circulatory water bath set at 18 °C for a period of 30 min and the percentage cooking loss was recorded. All samples were cut or compressed perpendicular to the muscle fiber direction at a crosshead speed of 3.33 and 1 mm s^{-1} for Warner- Bratzler (WB) and textural profile analysis (TPA) tests, respectively. A texture analyzer (TA-XT2, Stable Micro Systems, Godalming) was used in both tests. Four pieces of meat of 1 × 1 × 2.5 cm (height × width × length) were cut completely using a WB shear blade with a triangular slot cutting edge (1 mm thickness). Maximum shear force [33] was assessed by the higher peak of the force-time curve, which represents the maximum resistance of the sample to the cut. Four pieces of meat of 1 × 1 × 1 cm (height × width × length) were removed for TPA test according to methodology proposed by Bourne [34]. Hardness was measured by compressing to 80% with a probe of 19.85 cm^2 of surface contact. Hardness was determined as the maximal force of the first compression of the meat piece.

2.3. Protein extraction and quantification

Lyophilized beef powder (50 mg) was resuspended in 1.5 mL of lysis buffer (7 M urea; 2 M thiourea; 4% CHAPS; 10 mM DTT; and 2% Pharmalyte pH 3-10, GE

Healthcare, Uppsala) for 2 h at 25 °C. An aliquot of 250 µL was lysed using a Sonifier 250 (Branson, Danbury) by cycling. During this process, the sample vial was kept in an ice-water bath to prevent significant heating in the sample during sonication. Protein purification and extraction from crude cell lysates was carried out with the Clean-Up kit (GE Healthcare) as described in manufacturer´s indications [35]. The proteins were then resuspended in 250 µL of lysis buffer. Protein quantification was assessed for each extraction using the CB-X protein assay kit (G-Biosciences, St. Louis) according to manufacturer's recommendations for using a microplate reader. CB-X is an improved Bradford [36] assay, compatible with all commonly used buffers and conditions in protein isolation, which provides a quick estimation of protein concentration. The BSA protein standard was used to get a calibration curve.

2.4. 2-DE protein profiles

2-DE was performed according to Görg et al. [37] with some modification. 2-DE was carried out from 350 µg of total protein extract dissolved in lysis and rehydration (7 M urea, 2 M thiourea, 4% CHAPS, 0.002% bromophenol blue) buffers. Protein extracts were loaded into 24-cm-long ReadyStrip IPG Strips (Bio-Rad Laboratories, Hercules) with linear pH gradient of 4-7, together with 0.6% DTT and 1% IPG buffer (Bio-Rad Laboratories). The IEF was performed using a PROTEAN IEF cell system (Bio-Rad Laboratories). Gels were initially rehydrated for 12 h at 50 V. Rapid voltage ramping was subsequently applied to reach a total of 70 kVh. After IEF, strips were equilibrated for 15 min at room temperature in equilibration solution I (50 mM Tris pH 8.8, 6 M urea, 2% SDS, 30% glycerol and 1% DTT) and then with equilibration solution II (50 mM Tris pH 8.8, 6 M urea, 2% SDS, 30% glycerol and 4% iodoacetamide) under the

same conditions. Second dimension electrophoresis was run on 12% (w/v) SDS-PAGE gels using an Ettan DALTsix vertical slab gel system (GE, Healthcare) and Tris-glycine-SDS (50 mM Tris, 384 mM glycine and 0.2% SDS) as electrode buffer. Gels were run at a constant current of 32 mA at 25 °C.

2.5. Phosphoprotein staining with Pro-Q Diamond

The phosphoprotein-specific fluorescent dye Pro-Q Diamond phosphoprotein stain (Pro-Q DPS, Molecular Probes, Leiden) was used as a probe for the in-gel detection of phosphorylated polypeptides according to López-Pedrouso et al. [38]. 2-DE gels were treated with a fixation solution (45% methanol and 10% acetic acid, for 60 min) and washed twice with distilled water (15 min per wash). The gels were then incubated with two-fold water-diluted Pro-Q DPS (120 min), destained with destaining solution (50 mM sodium acetate and 20% ACN pH 4.0) four times (30 min per wash) to remove gel-bound nonspecific Pro-Q DPS and washed again twice with distilled water (5 min per wash). The Peppermint (Molecular Probes) phosphoprotein marker was added to protein extracts before 2-DE to validate the specificity of the recognition of phosphoproteins by Pro-Q DPS under our experimental conditions.

2.6. Total protein staining with SYPRO Ruby

The 2-DE gels were stained with SYPRO Ruby stain (Lonza, Rockland), for total protein density following the manufacturer's indications. Pro-Q DPS-stained gels were also post-stained with SYPRO Ruby. 2-DE gels stained for total protein (SYPRO Ruby) and phosphoprotein (Pro-Q DPS) detection were obtained for four biological replicates of DFD and control meats.

2.7. Image analysis

The 2-DE gel images from both Pro-Q DPS and SYPRO Ruby staining

methods were acquired using a Gel Doc XR+ system (Bio-Rad Laboratories). Image analysis of digitalized gels was performed through PDQuest Advanced software v. 8.0.1 (Bio-Rad Laboratories). 2-DE gels were matched across biological replicates and volume of each spot was quantitatively determined after background subtraction and normalization using total density of validated spots across all replicate gels. The p*I* and M_r of spots were determined from their position on the IEF-strips and standard molecular mass markers ranging from 15 to 200 kDa (Fermentas, Ontario), respectively.

2.8. Preparation of samples for MS

Spots of interest were excised from the gel taking care to maximize the protein-to-gel ratio. Only the most intense stained region at center of the spot was excised to avoid extracting an excess of gel matrix. Excised pieces were subjected to in-gel digestion with trypsin as described [39]. Briefly, excised spots were cut into pieces and washed with Milli-Q-water. Afterward, the pieces were dehydrated with ACN and dried in a vacuum centrifuge. Gel pieces were further digested with 1 µg/mL of trypsin (Promega, Madison) in 50 mM ammonium bicarbonate pH 8 to a final volume of 30 µL (overnight at 37 °C). For MALDI TOF/TOF MS analysis gel pieces were reduced with 10 mM DTT (Sigma-Aldrich, St. Louis) in 50 mM ammonium bicarbonate (Sigma-Aldrich) and alkylated with 55 mM iodoacetamide (Sigma- Aldrich) in 50 mM ammonium bicarbonate. The gel pieces were then rinsed with 50 mM ammonium bicarbonate in 50% methanol (HPLC grade, Scharlau, Barcelona), dehydrated by addition of ACN (HPLC grade) and dried in a SpeedVac. Modified porcine trypsin (Promega) was added to the dry gel pieces at a final concentration of 20 ng/µL in 20 mM ammonium bicarbonate, incubating them at 37 °C for 16 h. Peptides were extracted three times by 20 min incubation in 40 µL of 60% ACN in 0.5% HCOOH.

The resulting peptide extracts were pooled, concentrated in a SpeedVac and stored at −20 °C.

2.9. LC-MS/MS analysis

Peptide digests were acidified with acetic acid, cleaned on a C_{18} MicroSpin column (The Nest Group, South-borough) and analyzed by LC-MS/MS using a Agilent 1260 HPLC series system (Agilent Technologies, Santa Clara) coupled to an LIT-Velos mass spectrometer (Thermo Fisher, San Jose). Peptide separation was performed on a BioBasic-18 RP column (0.18 mm × 150 mm) (ThermoHypersil-Keystone, Bellefonte), using 0.15% acetic acid in Milli-Q-water and 98% ACN and 0.15% acetic acid as mobile phases A and B, respectively. A 90 min linear gradient from 5 to 40% B was used at a flow rate of 1.5 µL/min. The spray voltage used was 3.5 kV; N_2 flow, 8 arbitrary units, while the capillary temperature was 230 °C. Peptides were analyzed in the positive mode from 400 to 1600 amu (two microscans), followed by four data-dependent MS/MS scans (two microscans), using an isolation width of 3 amu and a normalized collision energy of 35%. Fragmented masses were set in dynamic exclusion for 2 min after the second fragmentation event, and singly charged ions were excluded from MS/MS analysis. MS/MS spectra were searched using SEQUEST (Proteome Discoverer 1.4 package, Thermo Fisher), against the *B. taurus* UniProt/SwissProt data- base (release 2013_10; 31.983 entries), which also included their respective decoy sequences. The following constraints were used for the searches: semi-tryptic cleavage with up to two missed cleavage sites and tolerances 1.2 Da for precursor ions and 0.5 Da for MS/MS fragment ions. The variable modifications allowed were methionine oxidation, carbamidomethylation of cysteine and acetylation of the N-terminus of the protein. The database search results were subjected to statistical analysis by Protein Discoverer

Peptide Confidence (v.4.0), choosing a False Discoverer Rate (FDR) threshold of 1-5%.

2.10. MALDI TOF/TOF MS analysis

MALDI TOF/TOF MS was used to verify protein identifications by LC-MS/MS. Dried samples were dissolved in 4 µL of 0.5% HCOOH. Equal volumes (0.5 µL) of peptide and matrix solution, consisting of 3 mg CHCA dissolved in 1 mL of 50% ACN in 0.1% TFA, were deposited onto a 384 Opti-TOF MALDI plate (Applied Biosystems, Foster City) using the thin layer method. Mass spectrometric data were obtained in an automated analysis loop using 4800 MALDI-TOF/TOF analyzer (Applied Biosystems). MS spectra were acquired in positive-ion reflector mode with a Nd:YAG, 355 nm wavelength laser, averaging 1000 laser shots, and at least three trypsin autolysis peaks were used as internal calibration. All MS/MS spectra were performed by selecting the precursors with a relative resolution of 300 (FWHM) and metastable suppression. Automated analysis of mass data was achieved using the 4000 Series Explorer Software

v. 3.5 (Applied Biosystems). PMF and peptide fragmentation spectra data of each sample were combined through the GPS Explorer Software v. 3.6 using Mascot software v. 2.1 (Matrix Science, Boston) to search against the *B. taurus* UniProt/ SwissProt database (release version 2015-02; February, 2015, 32.362 entries), with 30 ppm precursor tolerance, 0.35 Da MS/MS fragment tolerance, carbamidomethyl cysteine as fixed modification, oxidized methionine as variable modification and permitting one missed cleavage. All spectra and database results were manually inspected in detail using the above software. Protein scores greater than 56 were accepted as statistically significant ($p < 0.05$), and the identification was considered as positive when the protein score CI (confidence interval)

was above 98%. In the case of MSMS spectra, the total ion score CI was above 95%.

2.11. Statistical analysis

Standard statistical tests (Mann-Whitney U test, Spearman's correlation test, etc.) were performed using the IBM SPSS Statistics 20 (SPSS, Chicago) statistical software package. Non- parametric bootstrap confidence intervals (CIs) were obtained for the means of the observed spot volumes in DFD and control samples by the bias-corrected percentile method [40] using the software DIANA (Zapata C, unpublished). DIANA is a software package written in Visual Basic for population genetics data analysis. It uses random numbers from the standard multiplicative linear congruential generator implemented by Schrage [41] for generating the bootstrapped empirical distribution of the sample mean, a random number generator that gives very long sequences of "pseudo-random" numbers that have the appearance of randomness. For each set of *N* (= 4) estimates of spot volume, 2000 bootstrap samples of size *N* were drawn with replacement following a Monte Carlo algorithm. Bootstrap CIs were constructed from distribution of 2,000 bootstrap mean replications. The bias was corrected from the proportion of bootstrap mean replications less than the original estimate of the mean using the theoretical normal distribution [40].

The bootstrap-based statistical approach offers clear advantages in comparison with commonly used tests for testing differential abundance between samples: Student's t-test and Mann-Whitney U test [40,42]. The bootstrap algorithm uses the empirical distribution for the sample mean. In contrast, the t-test is based on the t-distribution (small samples) or normal distribution (large samples), which are parametric and theoretical

distributions that are generally only approached by the sample data. On the other hand, the Mann-Whitney is a non-parametric test but it cannot provide estimates of the magnitude of any difference because the observed data values are replaced by their ranks. Quantitative change in the volume of each protein spot from control to DFD samples was determined by the commonly used measure of "fold change" (*FC*). The *FC* is given by

$$FC = V_{DFD} / V_C$$

where V_{DFD} and V_C are the volume means for each spot across replicate gels in DFD and control meats, respectively. *FC*-values less than one were represented as their negative reciprocal. Therefore, *FC* ranges from - ∞ to + ∞. The change in the volume of each spot from control to DFD samples was also calculated using a new measure of relative change (*RC*), which is defined as follows

$$RC = DV / DV_{max}$$

where $DV = V_{DFD} - V_C$ is a measure of the differential volume between samples, and DV_{max} is the maximum observed value of *DV* over spots in the study. The *RC* measure has the advantage that it ranges between -1.0 and + 1.0 and takes a value of zero when there is no volume change.

2.12. Bioinformatic analyses

Gene ontology (GO) terms for each gene, inferred from electronic annotation or experimentally validated, were re- trieved with QuickGO (http://www.ebi.ac.uk/QuickGO/ ; Europe- an Bioinformatics Institute/EBI). Broader GO terms used to generate the pie charts were retrieved from the pre-existing GO slim generic subset (GO Consortium) by means of the Slimmer tool of AmiGO (http://amigo1.geneontology.org/cgi-bin/amigo/ slimmer; Species DB ALL, Evidence code ALL). For single enrichment of GO terms analysis we

used FatiGO [43],a specific software within the set of functional analysis tools of Babelomics 4 (http://v4.babelomics.org/) that took the list of terms associated with our bovine (*B. taurus*) genes of interest (idlist data type; Ensembl IDs) in different databases (GO biological process, GO molecular function, GO cellular component, KEGG and InterPro databases) and compared this list to the collection of terms associated with the rest of the genome. A two tailed Fisher's exact test was used to check for significant over-representation of annotations ($p < 0.05$). An analysis of predicted and known functional interactions between the identified proteins and other *B. taurus* proteins was performed using the STRING v9.1 software [44]. The "additional (white) nodes" and "interactors shown" parameters were set to 1 in order to obtain a protein-protein interaction network close to the proteins identified in our study.

2.13. Cluster analysis

Proteins that exhibited similar significant change in abundance from control to DFD meat were grouped into clusters by an agglomerative hierarchic cluster analysis. The unweighted pair-group method with arithmetic averaging (UPGMA) was used to cluster the proteins from the matrix of pairwise RC-values in absolute value. A UPGMA dendrogram was generated with NTSYSpc v. 2.1 software (Applied Biostatistics, Setauket).

3. Results

3.1. Identification of control and DFD meats

The determination of meat quality parameters in control (non-DFD) and DFD meat revealed that those samples selected in this study represent a biological material suitable for unraveling the proteome changes underlying the trans- formation of LT bovine muscle into DFD meat as a response to PSS. Table 1 shows mean values (±SE, standard error) of pH, color

parameters (L*, a* and b*), WHC (cooking loss) and texture (shear force and hardness) in control and DFD meat samples. Statistically significant differences between the two types of meat were detected across quality parameters assayed in this study by the one-tailed Mann-Whitney U test (p-value < 0.05). It can also be seen that the values of meat quality parameters fulfil all requirements of control and DFD meats [8]. Firstly, all biological replicates exhibited pH values lower than 6.0 in control meats while those of DFD meats were always higher than 6.0. Secondly, meat color as measured in trichromatic space was higher for L* and b* in the control cuts (highest luminosity) than in the DFD group (darkest color). Thirdly, the WHC was lower in control than in DFD group. Fourthly, meats from the control group showed the highest shear force and hardness as assessed by WB and TPA tests, respectively. In addition, there was a statistically significant negative relationship of L*, b*, shear force and hardness with pH ($r_s = -0.98$, n = 8; p < 0.01 for L*; $r_s = -0.91$,n = 8;p < 0.01, for b*; $r_s = -0.93$, n = 8; p < 0.01, for shear force; and $r_s = -0.73$, n = 8; p < 0.05, for hardness) as previously reported [9,45].

3.2. Identification of proteins linked to PSS by 2-DE and MS

Proteins extracted from DFD and control meat samples collected at 24 h post-mortem were separated using 2-DE. Sample lyophilization, protein extraction and electrophoretic methods used in the study resulted in good quality and highly reproducible 2-DE gel images (Supplementary Fig. 1). Representative 2-DE gel protein profiles for control and DFD meats are presented in Fig. 1. Detection, matching and measurement of the volume of protein spots across gels were assessed using PDQuest software. There was a set of 19 protein spots that showed greater intensity differences

between control and DFD groups. Specifically, 12 spots (designated as spots C1-12) were overrepresented in control meats, whereas the remaining 7 spots (spots D1-7) were overrepresented in DFD meats. Quantitative (i.e. different spot intensity between sample groups) and qualitative (i.e. presence/absence of a given spot in control or DFD meats) changes were found between the two types of samples. Table 2 gives the mean value (± SE) of the volume ($\times 10^{-2}$) of each protein spot in control and DFD samples along with their 95% and 99% bootstrap CIs. Difference of mean volumes between the two sample groups were found to be statistically significant ($p < 0.05$) for all protein spots, given that their 95% CIs did not overlap (spots with quantitative differences) or did not overlap zero (spots with qualitative differences). Differentially abundant protein spots between sample groups were selected for LC-MS/MS analysis. All protein spots were confidently identified by LC-MS/MS and identifications are listed in Table 3 (see Supplementary Table 1 for more detailed information). However, some identified proteins were subtracted from the final list of proteins analyzed in response to PSS for the following reasons. Firstly, an apparent fragmentation phenomenon was detected at six of the identified protein spots (AFG3L2, spot C1; CCBP2, spot C2; MYL6B-1, spot C7; CPS1, spot C8; MYL2-1, spot C-12; and CPS1, spot C12) from the comparison between the theoretical and the experimentally observed M_r on 2-DE gels. This is probably due to proteolytic degradation at 24 h post-mortem associated with cellular death and the meat aging process [46,47]. Secondly, three identifications (spots C3, C4 and C10) corresponded to uncharacterized proteins of *B. taurus*. Thirdly, the D4 protein spot contained a hypothetical protein (LOC767890). Therefore, the final list of selected spots for further analysis comprised a total of ten differentially abundant proteins in control

and DFD samples: MYL3, MYL6B, MYL2, TNNC2, STGAL1, ATP5B, TPI1, CFL2, MYLPF and MYLPF-1.

Protein identifications were validated from several other lines of evidence: MALDI-TOF/TOF MS analysis (Supplementary Table 2); close agreement between the theoretical and the 2-DE-based experimental M_r and p*I* (Table 3); and consistent results with previously reported protein identifications in LT bovine muscle based on 2-DE and MS [21,22].

Table 4 shows the strength of spot intensity changes between control and DFD meat as measured by *FC* and *RC* statistics. There can be seen that both statistics provided completely discrepant results about the relative magnitude of changed proteins in muscle conversion to DFD meat. The use of the *FC* measure has some inconveniences because of its range of variation (from −∞ to + ∞). *FC* gives values of - ∞/+ ∞ for qualitative changes between sample groups when the absence of a given spot can be due merely to the occurrence of protein amounts undetectable by 2-DE. In contrast, the measure *RC* allows us the joint analysis of spots with qualitative and quantitative changes under the same range of variation (i.e., from-1.0 to + 1.0). Consequently, the *RC* measure can provide more genuine information than *FC* to assess differential protein abundance in PSS response. Applying the *RC* statistic, MYL6B, MYL2, TNNC2 and MYL3 were found to be overrepresented (*RC* < 0) in control samples, whereas ATP5B, TPI1, CFL2, STGAL1, MYLPF and MYLPF-1 were overrepresented (*RC* > 0) in DFD samples (Table 4; Fig. 2). When proteins were ordered by the magnitude of *RC* scores it turned out that MYL6B and two MYLPF isoforms (MYLPF and MYLPF-1) underwent the sharpest decrease and increase, respectively, from control to DFD meats (Fig. 2). In particular, the MYLPF-1 protein exhibited the maximum difference of spot volume (DV_{mav}), highly represented in DFD meats (*RC* = + 1.0).

3.3. Phosphorylated fast skeletal light chain 2 (MYLPF) isoforms

Protein spots identified as MYLPF form part of a wider spot constellation with the same M_r but different p*I*s (Fig. 1), which suggests that they are probably MYLPF isoforms caused by post-translational modifications such as phophorylations and acetylations [48]. We first confirmed that indeed this spot constellation is formed by different MYLPF isoforms through post-translational modifications using MALDI TOF/TOF MS (Supplementary Table 3). In addition, the phosphoprotein- specific fluorescent dye Pro-Q DPS was used for in-gel detection of phosphorylated forms of MYLPF. The specificity of the recognition of phosphoproteins by Pro-Q DPS under our experimental conditions was validated using Peppermint phosphoprotein molecular weight standards (data not shown). Reference (SYPRO Ruby total protein stain) and phosphorylated (Pro-Q DPS phosphoprotein stain) MYLPF spot patterns on 2-DE gels obtained from control and DFD meat samples are shown in Fig. 3. It was found that two out of three MYLPF isoforms were phosphorylated in control samples, whereas four out of five isoforms were phosphorylated in DFD ones. The most alkaline protein spot in both types of samples (spot no. 1) was apparently the only unphosphorylated MYLPF isoform because it was not detected in gels with Pro-Q DPS. Note that the two additional protein spots found in DFD meat (spots no. 4 and no. 5) turned out to be highly phosphorylated MYLPF isoforms.

3.4. Bioinformatic and cluster analyses of identified proteins in PSS response

Fine-grained (Supplementary Table 4) and slim versions (Supplementary Fig. 2) of GO terms for each differentially abundant *B. taurus* protein were retrieved by means of Quick GO and the AmiGO Slimmer tool,

respectively, in order to categorize the identified proteins. According to Supplementary Table 4, the set of nine differentially abundant proteins were mainly involved in biological processes such as calcium ion binding and cardiac muscle morphogenesis/contraction, function as proteins that bind calcium ions and actin, and can be found at different locations, either outside cells such as the extracellular space and the cell membrane, or inside cells, such as the cytoskeleton, actin/tropomyosin complex, or nucleus. The same conclusions were drawn when upper level GO slim terms were used (Supplementary Fig. 2). Moreover, we also looked for significant overrepresentation of functional annotations in our set of nine genes regarding the distributions of functional terms from the rest of the bovine genome. Thus, FatiGO/Babelomics [43] single enrichment analysis displayed a significant ($p \leq 0.05$) enrichment of InterPro and GO molecular function database terms indicating calcium, cytoskeletal and actin binding (Supplementary Table 5). In addition, there was a significant ($p \leq 0.05$) enrichment in proteins linked to the following KEGG database pathways: Tight junction (bta04530), regulation of actin cytoskeleton (bta04810), focal adhesion (bta04510) and leukocyte transendothelial migration (bta04670).

STRING database revealed two groups of direct interactions between differently abundant proteins in PSS response: a major group of structural-contractile muscle proteins (MYL3, MYL6B, MYL2, MYLPF and TNNT1) and a minor group of only two proteins involved in structural-contractile functions (CFL2) and metabolism (TPI1) (Fig. 4). Note that TNNC2 was replaced by TNNT1 because STRING database found no proteins by this name on *B. taurus*. MYL3 exhibited the strongest interaction with MYL2, MYLPF and TNNT1 (thresh- old: 0.7; high confidence interval). Only two

proteins, namely ST6GAL1 and ATP5B, were not linked with the two interaction networks, and ATP5B was linked in an interactome at a first level (i.e. when a maximum of interaction with one protein of the proteome is searched by the STRING software). Using evidence only for co-expression of identified proteins from STRING database led to a single group of links between structural-contractile muscle proteins showing more solid levels of co-expression (Supplementary Fig. 3).

Cluster analysis gives an alternative perspective to STRING on the co-expression levels of the identified proteins based only on the information provided by this study. The UPGMA dendrogram obtained from differences in *RC* (in absolute value) between pairs of protein spots differentially abundant in control and DFD samples is shown in Fig. 5. Cluster analysis suggests the presence of two major clusters of related proteins and one outlier protein (protein MYLPF-1) distantly related to the other proteins. Thus, the outlier protein MYLPF-1 followed by the cluster made up of proteins MYLPF, MYL6B and MYL2 were the most differently abundant proteins according to the UPGMA dendrogram.

4. Discussion

In this study, we report the first evidence on the changes of the proteome landscape of LT bovine muscle in response to PSS. The combination of a diversity of proteomic tools led to identify proteins showing statistically significant abundance change in muscle conversion to DFD meat in the Rubia Gallega breed. The identified proteins can be grouped into two major functional categories: structural-contractile muscle proteins (MYL3, MYL6B, MYL2, MYLPF, TNNC2 and CFL2) and proteins involved in metabolism (TPI1, ATP5B and ST6GAL1). Most identified proteins and their modulation (increasing or decreas- ing) in response to PSS have a clear biological

549 significance.

550 Tenderness is considered to be one of the most important attributes
551 contributing to meat quality [19,49]. Current evidence suggests that longitudinal
552 and lateral sarcomere shrinkage, total collagen content, temperature, pH
553 and proteolysis play a central role in the tenderization process occurring
554 during post-mortem meat aging [49–51]. Sarcomere shortening during rigor
555 mortis development increases shear force with an increase in toughness during
556 the first 24 h post-mortem [49,50]. However, significant depletion of muscle
557 glycogen reserves associated with PSS response has a well-documented
558 effect on muscle fiber characteristics that control the tenderization phase
559 during the conversion of muscle to meat [1,51]. In this study, textural tests
560 showed that DFD meat of cattle affected by PSS was significantly tenderer at 24
561 h of aging than beef from normal cattle, as previously reported [45]. The
562 higher pH in DFD meat enhances electrostatic repulsion between the
563 myofibrillar proteins, which contributes to less lateral shrinkage of the
564 muscle fibers [51]. However, in-depth knowledge of proteome post-mortem
565 changes which occur upon slaughter of the animal is crucial for a better
566 understanding of the mechanisms controlling tenderness. A number of
567 studies have shown that structural proteins specific to the sarcomere,
568 including myosin light chains, and many other functionally diverse proteins
569 participate in meat tenderization [22,28–31,52]. But the available evidence
570 refers to biochemical changes underlying tenderization that occurs during
571 normal post-mortem aging of beef. It is noteworthy that meat affected by
572 PSS has particular characteristics and thereby tenderization processes may
573 be achieved by different biochemical mechanisms that in normal meat.

574 Our proteomic study revealed for the first time that several muscle myosin
575 light chains (MYL3 and MYL6B) and regulatory light chain 2 isoforms (MYL2

and MYLPF) participate in the conversion of cattle muscle to DFD meat in Rubia Gallega animals affected by PSS. All these proteins appeared to be involved in the main network of functionally associated proteins according to the STRING database. This is not a surprising result when the myosin is a major structural protein of the muscle sarcomere in association with actin and other contractile proteins. The MYL3, MYL6B and MYL2 proteins play important structural and functional roles by supporting the structure of the myosin neck region and fine-tuning the kinetics of the actin-myosin interaction [53]. We also found that levels of MYL6B, MYL2 and MYL3 were lower in DFD than in normal meat, probably because of a more intensive enzymatic degra- dation of myofibril structure, which can contribute to explain its tenderness differential. It has been pointed out that denatur- ation of the myosin heads can contribute to myofibrillar lateral shrinkage and reduction in its ability to bind water resulting in decreased WHC [51]. These effects might be outweighed in DFD meat by the regulatory role of MYL2 that triggers myofibril contraction by a Ca^{+2} and calmodulin-dependent myosin light chain kinase, meaning that decrease of MYL2 in DFD meat may reduce sarcomere shortening.

PSS is consequence of a rapid response of the animal in reaction to acute stressors that includes the activation and regulation of the autonomous nervous system and hypothalamic-pituitary- adrenal axis with effects on muscle proteins [1]. In addition to this, post-translational protein modification through phosphorylations has potential to be an important molecular mechanism of rapid response to acute stressors. Protein phosphorylation is a transient and revers- ible event that can change at very short intervals of time with a key regulatory role in a diversity of cellular processes [54]. Recent studies suggest that phosphorylation of muscle

603 proteins play an important role in the post-mortem muscle conversion to
604 meat and hence in meat quality [19,28]. In particular, phosphoproteomic
605 analysis of sarcoplasmic pro- teins in post-mortem porcine muscle revealed
606 high levels of phosphorylation in stress response proteins [55]. We found
607 that two phosphorylated fast skeletal myosin light chain 2 isoforms (i.e.
608 MYLPF and MYLPF-1) underwent the most intense relative change in
609 muscle conversion to DFD meat. They were the most phosphorylated fast
610 skeletal myosin light chain 2 isoforms present only in DFD meat. Our results
611 suggest, therefore, that these highly phosphorylated isoforms of MYLPF
612 are the most specific and sensitive biomarkers for PSS in the LT muscle of
613 the Rubia Gallega. It is well-recognized that MYL2 is highly phosphorylated
614 and that this phosphor- ylation is crucial for the regulation of MYL2 [56].
615 Levels of MYL2 phosphorylation around 30-40% have been reported in
616 humans and pig [53]. Interestingly, the N-terminal domain in the human
617 orthologue MYL2 contains a phosphorylation site that appears to have an
618 important modulatory role in striated muscle contraction [56]. It should also
619 be highlighted that increased levels of pH in DFD compared to normal meat
620 may run against the activity of acid phosphatases [55]. Further research is
621 required to assess whether phosphorylation of proteins is an extended
622 mechanism in PSS response through an intensive study of the muscle
623 phosphoproteome.

624 Our observations showed a decreased abundance of TNNC2 in DFD meat
625 which helps to explain its increased tenderness. TNNC forms part, together
626 with troponin T (TNNT) and troponin I (TNNI), of the regulatory protein complex of
627 the troponin that is central to muscle contraction in skeletal and cardiac
628 muscles [57]. The TNNC binds calcium ions and abolishes the inhibitory
629 action of troponin complex on actin filaments. In bovine muscle, the progress

of degradation of the myofibrillar TNNT subunit seems to be a good predictor of tenderization during normal post-mortem aging of beef [58]. We also found that CFL2 (cofilin, muscle isoform) was up-modulated in response to PSS. Cofilin is an isoform of the actin depolymeration factor family involved in regulating the actin cytoskeleton and in other multiple facets of cellular biology [59]. It has the ability to bind G- and F-actin in a1:1 ratio of cofilin to actin and is the major component of intranuclear and cytoplasmic actin rods. CFL2 is a skeletal- muscle specific protein localized to the thin filaments/cytoskeleton, cytoplasm and nucleus. It controls reversibly actin polymerization and depolymerization in a pH-sensitive manner, with maximal depolymerization at pH 8.0 and almost abolished at pH < 7.0 [60]. This means that the normal post-mortem pH decline from 7.0 to 5.5 due to lactic acid accumulation will favor actin polymerization and sarcomere structure contraction, while in DFD meat the higher pH (above 6.0) could sustain better cofilin-dependent F-actin depolymerization, contributing to higher WHC and improved tenderness.

Non-structural proteins can also be associated with tenderization in response to stress in cattle. Recent evidence shows that genes involved in immune response and regulation of metabolism in Angus cattle were associated with variation in beef tenderness induced by acute stress, using cDNA microarray and quantitative real-time PCR expression analysis [61]. We found increased levels of glycolytic (TPI1), mitochondrial membrane (ATP5B) and glycosyltransferase (ST6GAL1) proteins in DFD as compared to normal meats. Higher levels of glycolytic enzymes such as TPI, an enzyme that catalyzes the interconversion of dihydroxyacetone phosphate and glyceraldehyde 3-phosphate, seem to be related to meat tenderness in cattle and porcine muscles [29]. A prolonged ATP generation via glycolysis

contributes to both lactate and hydrogen ion accumulation. As above mentioned, this increases in hydrogen ions reduces electrostatic repulsion between the myofibrillar proteins and contributes to lateral shrinkage of the muscle fibers. Nevertheless, augmented levels of both TPI and CFL2 might lead to a higher WHC and tenderness in DFD meat by affecting the intracellular sodium concentration and osmolality. In fact, STRING database and cluster analyses disclosed that CFL2 and TPI1 were included in a minor cluster of associated proteins and formed part of a sub-cluster with a similar level of relative change in the conversion of normal to DFD meat, respectively. It is known that production of ATP by glycolysis in muscle supports ATP consumption by ion pumps located in the plasma mem- brane such as the Na^+/K^+-ATPase [62–64]. Interestingly, an interaction at the plasma membrane between the Na^+/K^+-ATPase and the phosphorylated form of cofilin-1 (the non-muscle counterpart of CFL2) complexed with TPI has been described, and this interaction serves to feed glycolytic ATP for the Na^+/K^+-ATPase pump [65].

5. Conclusions

Our study showed that the proteome of the LT bovine muscle of the Rubia Gallega breed underwent noticeable changes in response to PSS. Specifically, significant differential levels of expression of ten structural-contractile skeletal muscle proteins and metabolic proteins were found to be associated with PSS. Most proteome changes were represented by a group of strongly interacting structural proteins involving different myosin light chain isoforms and troponin C type 2. Our results also suggest that changes in the proteome linked to PSS involve not only quantitative differences at the level of protein abundance, but also pos-translational protein modifications through phosphorylations. In particular, highly phosphorylated fast skeletal myosin light chain 2 isoforms appeared to be

the most informative biomarkers linked to PSS response in Rubia Gallega. The functions of the identified proteins contribute to a better understanding of the increased tenderness and WHC in meat from animals affected by PSS. In addition, the results presented herein suggest that the new measure of relative change is more efficient than the usual measure of fold change to reliably compare differential protein abundance between sample groups. Finally, it is widely recognized that a diversity of endogenous and exogenous animal factors affect PSS response. Further systematic follow-up studies are clearly required, therefore, to unravel the entire sub-proteome involved in the molecular mechanisms associated with PSS in cattle.

Supplementary data to this article can be found online at http://dx.doi.org/10.1016/j.jprot.2015.03.029.

Conflict of interest

The authors declare no conflict of interest.

Acknowledgments

The authors would like to thank the anonymous reviewers for their valuable comments and suggestions to improve the quality of the article.

References

Ferguson DM, Warner RD. Have we underestimated the impact of pre-slaughter stress on meat quality in ruminants? Meat Sci 2008;80:12–9.

711 Miranda-de la Lama GC, Villarroel M, María GA. Livestock transport from
712 the perspective of the pre-slaughter logistic chain: a review. Meat Sci
713 2014;98:9–20.
714 Grandin T. Auditing animal welfare at slaughter plants. Rev Meat Sci
715 2010;86:56–65.
716 Grandin T. Asseessment of stress during handling and transport. J Anim
717 Sci 1997;75:249–75.
718 Lawrie RA, Ledward DA. Lawrie's meat science. Cambridge: Woodhead
719 Publishing Limited; 2006.
720 Warriss PD. Meat science: An introductory text. Wallingford & New York: CABI
721 Publishing; 2006.
722 Terlouw EMC, Arnould C, Auperin B, Berri C, Le Bihan-Duva E, Deiss V, et al.
723 Pre-slaughter conditions, animal stress and welfare: Current status and
724 possible future research. Animal 2008;2:1501–17.
725 Adzitey F, Nurul H. Pale soft exudative (PSE) and dark firm dry (DFD) meats:
726 causes and measures to reduce these incidences – a mini review. Int Food
727 Res J 2011;18:11–20.
728 Abril M, Campo MM, Önenç A, Sañudo C, AlbertíP, Negueruela AI. Beef
729 colour evolution as a function of ultimate pH. Meat Sci 2001;58:69–78.
730 Purchas RW, Aungsupakorn R. Further Investigations into the relationship
731 between ultimate pH and tenderness for beef samples from bulls and
732 steers. Meat Sci 1993;34:163–78.
733 Newton KG, Gill CO. The microbiology of DFD fresh meats: A review. Meat
734 Sci 1981;5:223–32.
735 Viljoen HF, De Kock HL, Webb EC. Consumer acceptability of dark, firm and
736 dry (DFD) and normal pH beef steaks. Meat Sci 2002;61:181–5.
737 Moore MC, Gary GD, Hale DS, Kerth CR, Griffin DB, Savell JW, et al. National

738 Beef Quality Audit–2011: In-plant survey of targeted carcass
739 characteristics related to quality, quantity, value, and marketing of fed
740 steers and heifers. J Anim Sci 2012;90:5143–51.
741 Smith GC, Savell JW, Dolezal HG, Field TG, Gill DG, Griffin DB, et al. The
742 National Beef Quality Audit. Colorado State University. Fort Collins;
743 Oklahoma State University, Stillwater. Texas: A&M University. College
744 Station; 1995.
745 Bourguet C, Deiss V, Gobert M, Durand D, Boissy A, Terlouw EMC.
746 Characterising the emotional reactivity of cows to understand and predict
747 their stress reactions to the slaughter procedure. Appl Anim Behav Sci
748 2010;125:9–21.
749 Averós X, Martín S, Riu M, Serratosa J, Gosálvez LF. Stress response of
750 extensively reared young bulls being transported to growing-finishing farms
751 under Spanish summer commercial conditions. Livest Sci 2008;119:174–
752 82.
753 Frylinck L, Strydom PE, Webb EC, du Toit E. Effect of South African beef
754 production systems on post-mortem muscle energy status and meat
755 quality. Meat Sci 2013;93:827–37.
756 D'Alessandro A, Zolla L. Food safety and quality control: hints from proteomics.
757 Food Technol Biotech 2012;50:275–85.
758 Paredi G, Raboni S, Bendixen E, de Almeida AM, Mozzarelli A. "Muscle to meat"
759 molecular events and technological transformations: the proteomics
760 insight. J Proteomics 2012; 75:4275–89.
761 Bendixen E. The use of proteomics in meat science. Meat Sci
762 2005;71:138–49.
763 Bouley J, Chambon C, Picard B. Mapping of bovine skeletal muscle
764 proteins using two-dimensional gel electrophoresis and mass

765 spectrometry. Proteomics 2004;4:1811–24.
766 Laville E, Sayd T, Morzel M, Blinet S, Chambon C, Lepetit J, et al. Proteome
767 changes during meat aging in tough and tender beef suggest the
768 importance of apoptosis and protein solubility for beef aging and
769 tenderization. J Agric Food Chem 2009;57:10755–64.
770 Shibata M, Matsumoto K, Oe M, Ohnishi-Kameyama M, Ojima K, Nakajima I,
771 et al. Differential expression of the skeletal muscle proteome in grazed
772 cattle. J Anim Sci 2009;87:2700–8.
773 Marcos B, Mullen AM. High pressure induced changes in beef muscle
774 proteome: Correlation with quality parameters. Meat Sci 2014;97:11–20.
775 Bjarnadóttir SG, Hollung K, Faergestad EM, Veiseth-Kent E. Proteome
776 changes in bovine *longissimus thoracis* muscle during the first 48 h
777 postmortem: shifts in energy status and myofibrillar stability. J Agric Food
778 Chem 2010;58:7408–14.
779 Kim NK, Cho S, Lee SH, Park HR, Lee CS, Cho YM, et al. Proteins in
780 *longissimus* muscle of Korean native cattle and their relationship to meat
781 quality. Meat Sci 2008;80:1068–73.
782 Suman SO, Rentfrow G, Nair MN, Joseph P. 2013 EARLY CAREER
783 ACHIEVEMENT AWARD – Proteomics of muscle- and species-specificity in
784 meat color stability. J Anim Sci 2014;92: 875–82.
785 D'Alessandro A, Marrocco C, Rinalducci S, Mirasole C, Failla S, Zolla L.
786 Chianina beef tenderness investigated through integrated Omics. J
787 Proteomics 2012;75:4381–98.
788 Ouali A, Gagaoua M, Boudida Y, Becila S, Boudjellal A, Herrera-Mendez
789 CH, et al. Biomarkers of meat tenderness: present knowledge and
790 perspectives in regards to our current understanding of the mechanisms
791 involved. Meat Sci 2013;95: 854–70.

792 Guillermin N, Bonnet M, Jurie C, Picard B. Functional analysis of beef
793 tenderness. J Proteomics 2011;75:352–65.
794 Zapata I, Zerby HN, Wick M. Functional proteomic analysis predicts beef
795 tenderness and the tenderness differential. J Agric Food Chem
796 2009;57:4956–63.
797 Carpentier SC, Dens K, Van den Houwe I, Swennen R, Panis B. Lyophilization,
798 a practical way to store and transport tissues prior to protein extraction for
799 2-DE analysis? Pract Proteomics 2007;1:64–9.
800 MØller A. Analysis of Warner Bratzler shear force pattern with regard to
801 myofibrillar and connective tissue components of tenderness. Meat Sci
802 1980;5:247–60.
803 Bourne MC. Texture profile analysis. Food Technol 1978;32: 62–6.
804 Healthcare GE. Handbook: 2-D electrophoresis using inmobilized pH
805 gradients, principles & methods. Piscataway: GE Healthcare; 2004.
806 Bradford MM. A rapid and sensitive method for the quantitation of
807 microgram quantities of protein utilizing the principle of protein-dye binding.
808 Anal Chem 1976;72:248–54.
809 Görg A, Obermaier C, Boguth G, Harder A, Scheibe B, Wildgruber R, et al.
810 The current state of two-dimensional electrophoresis with immobilized pH
811 gradients. Electrophoresis 2000;21:1037–53.
812 López-Pedrouso M, Alonso J, Zapata C. Evidence for phosphorylation of
813 the major seed storage protein of the common bean and its phosphorylation-
814 dependent degradation during germination. Plant Mol Biol 2014;84:415–28.
815 Jensen ON, Wilm M, Shevchenko A, Mann M. Sample preparation methods
816 for mass spectrometric peptide mapping directly from 2-DE gels. Methods
817 Mol Biol 1999;112: 513–30.
818 Efron B. The jackknife, the bootstrap and other resampling plans. CBMS-

NSF Regional Conference Series in Applied Mathematics No. 38. Philadelphia: Society for Industrial and Applied Mathematics; 1982.

Schrage L. A more portable Fortran random number generator. ACM Trans Math Softw 1979;5:132–8.

Sokal RR, Rohlf FJ. Biometry. New York: W.H. Freeman and Company; 2012.

Al-Shahrour F, Díaz-Uriarte R, Dopazo J. FatiGO: A web tool for finding significant associations of Gene Ontology terms with groups of genes. Bioinformatics 2004;20:578–80.

Franceschini A, Szklarczyk D, Frankild S, Kuhn M, Simonovis M, Roth A, et al. STRING v9.1: protein-protein interaction networks with increased coverage and integration. Nucleic Acids Res 2013;41:D808–15.

Silva JA, Patarata L, Martins C. Influence of ultimate pH on bovine meat tenderness during ageing. Meat Sci 1999;52: 453–9.

Taylor RG, Geesink GH, Thompson VF, Koohmaraie M, Goll DE. Is Z-disk degeneration responsible for postmortem tenderization? J Anim Sci 1995;73:1351–67.

Geesink GH, Koohmaraie M. Effect of calpastatin on degradation of myofibrillar proteins by μ-calpain under postmortem conditions. J Anim Sci 1999;77:2685–92.

Zhu K, Zhao J, Lubman DM, Miller FR, Barder TJ. Protein p*I* shifts due to posttranslational modifications in the separation and characterization of proteins. Anal Chem 2005; 77:2745–55.

Maltin C, Balcerzak R, Tilley R, Delday M. Determinants of meat quality: tenderness. Proc Nutr Soc 2003;62:337–47.

Koohmarie M. Biochemical factors regulating the toughening and tenderization processes of meat. Meat Sci 1996:S193–201.

Pearce KL, Rosenvold K, Andersen HJ, Hopkins DL. Water distribution and

mobility in meat during the conversion of muscle to meat and ageing and the impacts on fresh meat quality attributes − a review. Meat Sci 2011;89:111–24.

Anderson MJ, Lonergan SM, Huff-Lonergan E. Myosin light chain 1 release from myofibrillar fraction during post-mortem aging is a potential indicator of proteolysis and tenderness of beef. Meat Sci 2012;90:345–51.

Doroszko A, Polewicz D, Cadete VJJ, Sawicka J, Jones M, Szczesna-Cordary D, et al. Neonatal asphyxia induces the nitration of cardiac myosin light chain 2 (MLC2) which is associated with cardiac systolic dysfunction. Shock 2010;34: 592–600.

Schubert P, Hoffman MD, Sniatynski MJ, Kast J. Advances in the analysis of dynamic protein complexes by proteomics and data processing. Anal Bioanal Chem 2006;386:482–93.

Huang H, Larsen MR, Karlsson AH, Pomponio L, Costa LN, Lametsch R. Gel-based phosphoproteomics analysis of sarcoplasmic proteins in post-mortem porcine muscle with pH decline rate and time differences. Proteomics 2011;11: 4063–76.

Szczesna-Cordary D. Regulatory light chains of striated muscle myosin. Structure, function and malfunction. Curr Drug Targets Cardiovasc Haematol Disord 2003;3:187–97.

Pearson AM, Young RB. Muscle and Meat Biochemistry. San Diego: Academic Press; 1989.

Penny IF, Dransfield E. Relationship between toughness and troponin T in conditioned beef. Meat Sci 1979;3:135–41.

Munsie LN, Desmond CR, Truant R. Cofilin nuclear-cytoplasmic shuttling affects cofilin-actin rod formation during stress. J Cell Sci 2012;125:3977–88.

Papalouka V, Arvanitis DA, Vafiadaki E, Mavroidis M, Papadodima SA,

Spiliopoulou CA, et al. Muscle Lim Protein interacts with cofilin 2 and regulates F-actin dynamics in cardiac and skeletal muscle. Mol Cell Biol 2009;29:6046–58.

Zhao C, Tian F, Yu Y, Luo J, Mitra A, Zhan F, et al. Functional genomic analysis of variation on beef tenderness induced by acute stress in Angus cattle. Comp Funct Genom 2012;2012: 756284.

Clarke FM, Masters CJ. On the association of glycolytic enzymes with structural proteins of skeletal muscle. Biochim Biophys Acta 1975;381:37–46.

Campbell JD, Paul RJ. The nature of fuel provision for the Na+, K(+)-ATPase in porcine vascular smooth muscle. J Physiol 1992;447:67–82.

Cantiello HF. Actin filaments stimulate the Na(+)/K(+)-ATPase. Am J Physiol 1995;269:F637–43.

Jung J, Yoon T, Choi EC, Lee K. Interaction of cofilin with triose-phosphate isomerase contributes glycolytic fuel for Na, K-ATPase via Rho-mediated signaling pathway. J Biol Chem 2002;277:48931–7.

CAPTION TO FIGURES

Fig. 1 – Representative 2-DE gel protein profiles of control (top) and DFD (bottom) meat samples from the *longissimus thoracis* bovine muscle. Protein spots with significantly different abundance between the two groups of samples are marked and numbered. The numbers indicated in the gels correspond to the Tables 2–4.

Fig. 2 – Relative change (*RC*) in the volume of protein spots with significantly different abundance in the *longissimus thoracis* bovine muscle conversion to DFD meat.

Fig. 3 – Representative 2-DE gel sections for protein spots of fast skeletal myosin regulatory light chain 2 (MYLPF) isoforms from control (left) and DFD (right) meat samples of the *longissimus thoracis* bovine muscle. MYLPF isoforms stained for total protein (SYPRO Ruby; top) and phosphorylated protein (Pro-Q DPS, bottom) are shown. Isoforms with the same number are located on the same position (p*I* and M_r) across gels stained for total and phosphorylated protein.

Fig. 4 – Protein-protein interaction networks of differentially abundant stress-related protein spots in the *longissimus thoracis* bovine muscle, according to STRING confidence view. The network nodes (circles) are proteins, the edges represent known or predicted functional associations and line thickness is a rough indicator for the strength of the association (threshold: 0.4, medium confidence interval).

Fig. 5 – Dendrogram derived from unweighted pair-group method with arithmetic averaging (UPGMA) cluster analysis based on the matrix of pairwise differences in the relative change (*RC*) of protein spots (in absolute value) with significantly different abundance in the *longissimus thoracis*

bovine muscle conversion to DFD meat.

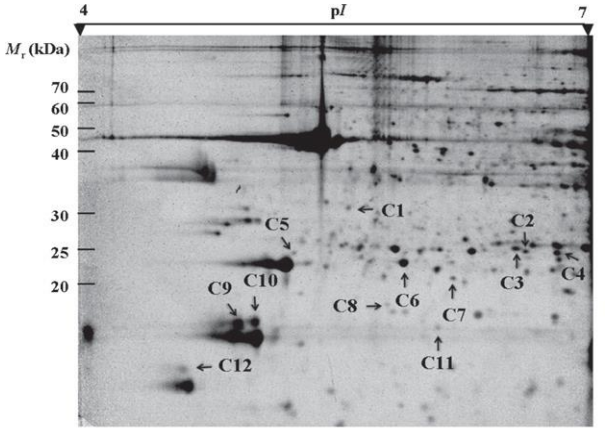

CONTROL (non-DFD)

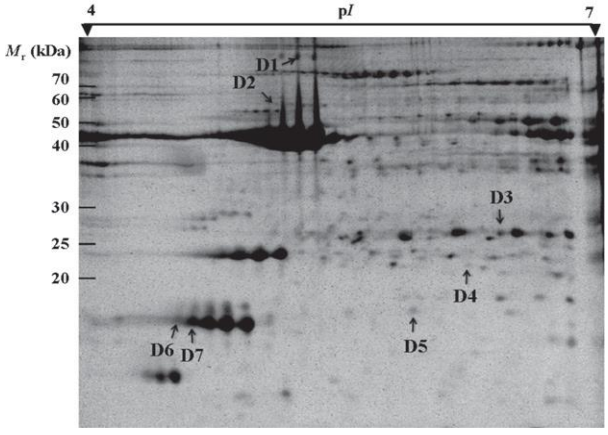

Figure 1

924

925 **Figure 2.**

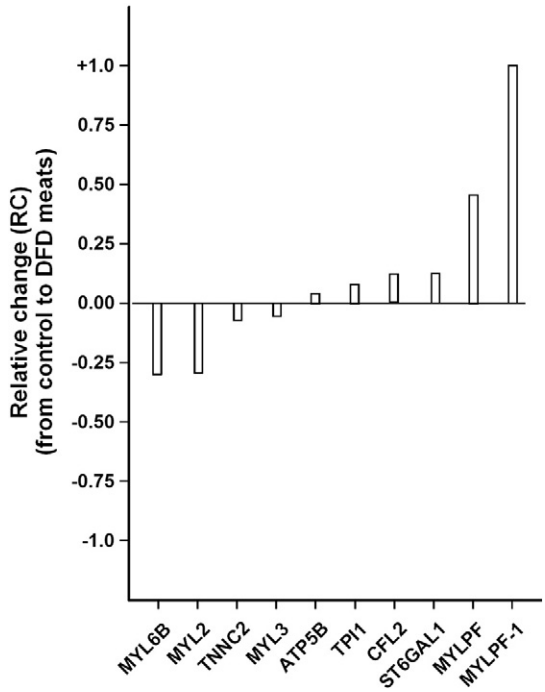

926

927

928 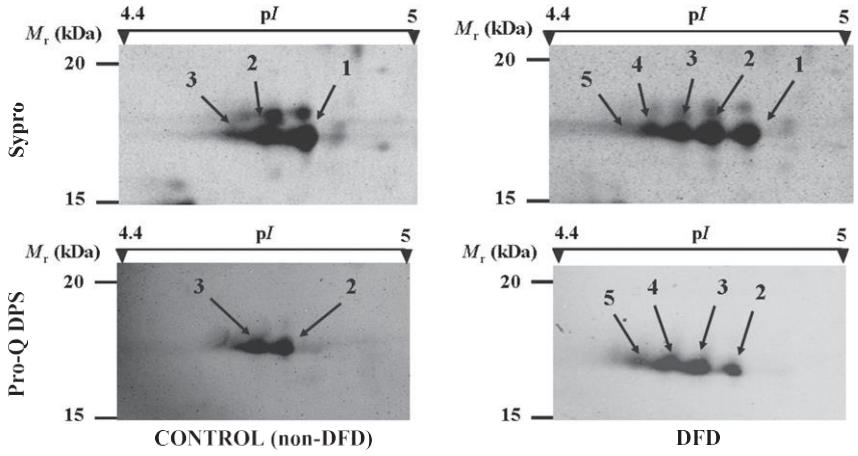

929 **Figure 3.**

930

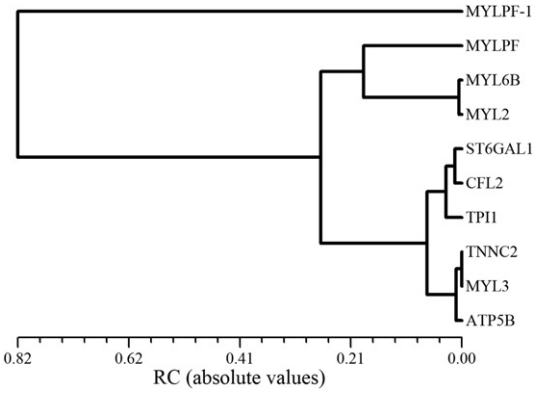
MYLPF-1
MYLPF
MYL6B
MYL2
ST6GAL1
CFL2
TPI1
TNNC2
MYL3
ATP5B
0.82
0.62
0.41
0.21
0.00
RC (absolute values)

Figure 4.

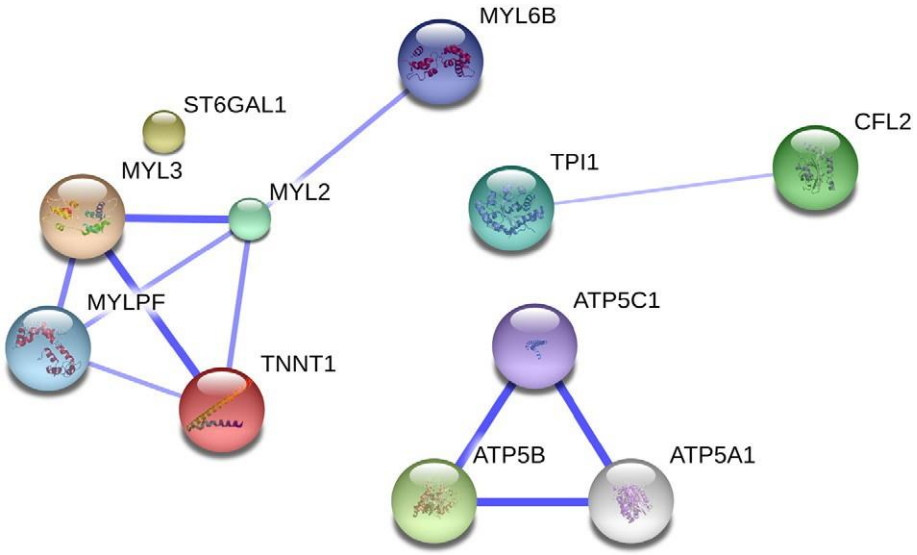
MYL6B
ST6GAL1
CFL2
MYL3
TPI1
MYL2
MYLPF
ATP5C1
TNNT1
ATP5B
ATP5A1

Figure 5.

Table 1 – Values of meat quality parameters (pH, color, water holding capacity and textural parameters) in control (non-DFD) and DFD samples from the longissimus thoracis bovine muscle.

Parameters	Control[a]	DFD[a]	p-value[b]
pH	5.61 ± 0.01	6.37 ± 0.13	0.01
Color:			
Luminosity (L*)	41.8 ± 1.61	35.8 ± 1.37	0.01
Redness (a*)	13.4 ± 0.63	9.62 ± 1.73	0.07
Yellowness (b*)	14.8 ± 0.29	8.01 ± 0.71	0.01
Water holding capacity:			
Cooking loss (%)	22.7 ± 3.50	12.2 ± 1.02	0.01
Textural / WB-test:			
Shear force (kg cm^{-2})	3.31 ± 0.42	1.89 ± 0.64	0.02
Textural/TPA-test:			
Hardness (kg)	5.93 ± 0.61	4.94 ± 0.34	0.02

[a] Data are means (± standard error) from four biological replicates; [b] p, probability by one-tailed Mann-Whitney U test.

Table 2 – Volume (× 10−2) of differentially abundant protein spots in control (non-DFD) and DFD meat samples assessed by PDQuest software.

Spot code[a]	Control			DFD			p-value[c]
	Volume[b]	95% bootstrap CI (CL, CU)[c]	99% bootstrap CI (CL, CU)[c]	Volume[b]	95% bootstrap CI (CL, CU)	99% bootstrap CI (CL, CU)	
C1	4.55 ± 0.96	3.25, 6,57	3.22, 7.30	1.76 ± 0.43	0.93, 2.49	0.90, 2.49	<0.01
C2	1.72 ± 0.81	0.39, 3.30	0.19, 3.54	0.00	–	–	<0.01
C3	7.15 ± 1.81	4.93, 10.7	4.15, 12.1	0.00	–	–	<0.01
C4	2.96 ± 0.90	1.04, 4.36	0.99, 4.61	0.00	–	–	<0.01
C5	2.16 ± 0.46	1.33, 2.82	1.21, 3.01	0.00	–	–	<0.01
C6	13.6 ± 8.41	4.44, 30.8	4.38, 38.8	2.40 ± 0.71	1.57, 3.77	1.56, 4.50	<0.05
C7	3.48 ± 0.82	2.37, 4.69	2.26, 4,80	0.00	–	–	<0.01
C8	4.41 ± 0.46	3.59, 5.09	3.13, 5.14	2.44 ± 0.65	1.25, 3.34	0.62, 3,43	<0.05
C9	18.7 ± 3.24	14.1, 24.3	12.4, 24.4	7.81 ± 1.83	5.67, 11.5	5.54, 11.6	<0.01
C10	16.2 ± 3.96	10.6, 24.6	10.5, 27.4	4.21 ± 0.32	3.77, 4.87	3.67, 5.09	<0.01
C11	2.27 ± 0.94	0.71, 4.12	0.62, 4.74	0.00	–	–	< 0.01
C12	5.01 ± 0.66	3.79, 5.91	3.63, 6.06	0.91 ± 0.70	0.10, 2.34	0.09, 2.99	< 0.01
D1	0.28 ± 0.28	0.00, 0.56	0.00, 0.56	5.60 ± 3.31	2.29, 8.90	2.29, 8.90	< 0.01
D2	0.62 ± 0.19	0.25, 0.87	0.06, 0.90	2.35 ± 0.49	1.67, 3.34	1.50, 3.66	< 0.01
D3	3.03 ± 0.12	2.80, 3.25	2.80, 3.25	6.83 ± 2.61	3.40, 12.3	2.93, 12.3	< 0.05
D4	0.00	–	–	1.64 ± 0.29	1.33, 2.23	1.30, 2.50	< 0.01
D5	0.00	–	–	4.72 ± 1.34	2.96, 7.53	2.71, 8.58	< 0.01
D6	0.00	–	–	18.1 ± 6.15	5.58, 26.0	5.58, 27.3	< 0.01
D7	0.00	–	–	38.1 ± 14.5	16.3, 59.9	8.11, 63.3	< 0.01

[a] Gel position of assigned spots is shown in Fig. 1. [b] Data are means ± standard error. [b] CI, Confidence interval; CL, lower bound; CU, upper bound. [c] Statistically significant ($p < 0.05$) differences between sample groups were found after correction for multiple testing by the sequential Bonferroni technique [42].

Table 3 – Identification by LC-MS/MS of 2-DE protein spots differentially abundant in control and DFD meat samples from the longissimus thoracis bovine muscle

Spot code	M_r (kDa) Observed/ expected	pI Observed/ expected	Protein	Abbrev.	Accesion No. (Uniprot)	Coverage (%)	No. of non-redundant peptides	Spectral counts
C1	29.2/89.4	5.30/8.83	AFG3-like protein 2	AFG3L2	Q2KJI7	7.95	6	15
C2	25.0/43.6	6.59/8.98	Chemokine binding protein 2	CCBP2	Q58CW9	15.36	5	12
C3	25.7/–	6.51/–	Uncharacterized protein				4	4
C4	23.5/–	6.97/–	Uncharacterized protein				5	5
C5	22.7/21.9	5.02/5.00	Myosin light chain 3	MYL3	P85100	43.21	4	11
C6	21.1/23.4	5.69/5.40	Myosin light chain 6B, alkali, smooth muscle and non-muscle	MYL6B	Q148H2	17.06	3	76
C7	20.0/23.4	6.03/5.40	Myosin, light chain 6B, alkali, smooth muscle and non-muscle	MYL6B-1	Q148H2	24.64	5	10
C8	18.5/164.7	5.59/6.28	Carbamoyl-phosphate synthase	CPS1	F1ML89	3.20	4	9
C9	18.1/19.0	4.86/4.88	Myosin regulatory light chain 2, ventricular/cardiac muscle isoform	MYL2	F1ME15	52.94	9	221
C10	18.2/–	4.90/–	Uncharacterized protein				3	3
C11	17.8/18.2	5.91/4.06	Troponin C type 2, fast	TNNC2	G3MZK7	44.34	4	15
C12	16.3/19.0	4.70/4.83	Myosin regulatory light chain 2, ventricular/cardiac muscle isoform	MYL2-1	F1ME15	23.49	3	16
	16.3/164.7	4.70/6.28	Carbamoyl-phosphate synthase 1	CPS1	F1ML89	2.46	3	11
D1	86.7/28.4	5.04/9.84	Beta-galactoside alpha-2,6-sialyltransferase 1	ST6GAL1	Q2KIW7	20.47	4	18
D2	52.6/56.3	4.98/5.15	ATP synthase subunit beta, mitochondrial	ATP5B	P00829	17.42	6	24
D3	26.1/26.7	6.25/6.45	Triosephosphate isomerase	TPI1	Q5E956	16.46	3	53
D4	20.0/22.9	6.03/12.2	LOC767890 protein	LOC767890	Q29RN5	19.16	4	7
D5	17.8/18.7	5.63/7.66	Cofilin-2	CFL2	Q148F1	26.50	4	11
D6	17.7/19.0	4.74/4.88	Myosin regulatory light chain 2, fast skeletal muscle isoform	MYLPF	Q0P571	15.88	3	5
D7	17.6/19.0	4.77/4.88	Myosin regulatory light chain 2, fast skeletal muscle isoform	MYLPF-1	Q0P571	34.12	4	18

Table 4 – Fold change (FC) and relative change (RC) of spot volume on 2-DE gels for differentially abundant proteins in control and DFD meats.

Spot code	Protein name	Fold change (FC)	Relative change (RC)
C5	Myosin light chain 3 (MYL3)	– ∞	-0.057
C6	Myosin light chain 6B, alkali, smooth muscle and non-muscle (MYL6B)	-5.68	-0.294
C9	Myosin regulatory light chain 2, ventricular/cardiac muscle isoform (MYL2)	-2.40	-0.286
C11	Troponin C type 2, fast (TNNC2)	– ∞	-0.060
D1	Beta-galactoside alpha-2,6-sialyltransferase 1 (ST6GAL1)	+20.00	+0.140
D2	ATP synthase subunit beta, mitochondrial (ATP5B)	+3.79	+0.045
D3	Triosephosphate isomerase (TPI1)	+2.25	+0.100
D5	Cofilin-2 (CFL2)	+ ∞	+0.124
D6	Myosin regulatory light chain 2, fast skeletal muscle isoform (MYLPF)	+ ∞	+0.475
D7	Myosin regulatory light chain 2, fast skeletal muscle isoform (MYLPF-1)	+ ∞	+1.000